IJNRD.ORG ISSN : 2456-4184
INTERNATIONAL JOURNAL OF NOVEL RESEARCH AND DEVELOPMENT (IJNRD) | IJNRD.ORG
An International Open Access, Peer-reviewed, Refereed Journal

The Studies on the Structural, Dielectric and Optical Bandgap Characteristics of $PbTiO_3$ Perovskite Material

[1]Kapil Vaishnave[1#] and Dr. Rajesh Kumar Katare[1]
[1]Research Scholar, Dept. of Physics, SAGE University-Indore (M.P.)-India
Professor, Dept. of Physics, SAGE University-Indore (M.P.)-India
Karpilvaishnav23@gmail.com

Abstract: The perovskite material of lead titanate ($PbTiO_3$) has reported. The material was prepared by employing solid state reaction (SSR) technique known as double calcination method of SSR route. The sample was examined by X-ray diffraction technique to throw light on the phase formation and the acquired crystal structure. It was found to have acquired the tetragonal structure (P4mm). The XRD spectrum analysis reveals the purity of tetragonal phase as extra XRD peaks are absent within the limits of the experiment. Sharp peaks indicate higher average particle size ≈ 96nm estimated using classical Debye-Scherer's formula. The dielectric properties in terms of applied ac field reveal relatively low dielectric constant and hence the dielectric loss character of the sample under investigation. Attributed to this character, $PbTiO_3$ is widely used in multilayer capacitor, resonators, and ultrasonic transducers. The ac conductivity was witnessed to be very small revealing its insulator nature. The optical bandgap has been estimated to be ≈ 3.16 eV using DRS-UV-Vis spectroscopy and this wide band gap is feasible in opto-electronic device applications. The ferroelectric nature was experimented via P-E hysteresis loop measurement and it was found the saturation is relatively good but remnant polarization value is low with leakage in the sample.

Keywords: Perovskites; Lead Titanate; Crystal Structure; Relative Permittivity; Optical Bandgap

---

INTRODUCTION

Perovskites such as barium titanate ($BaTiO_3$) and lead titanate ($PbTiO_3$) are exceptionally better dielectric, ferroelectric and piezoelectric materials as a result of these features they have versatile applications in thin-film capacitors, actuators, electronic transducers, pyroelectric sensors, high-k dielectrics, and nonlinear optics etc. These perovskite ferroelectrics with perovskite structures (ABO3), are frequently researched ferroelectric oxides [1, 2]. These materials inherit superior ferroelectric, piezoelectric, pyroelectric, and dielectric qualities that earned them recognition on a global scale. Perovskites are the most technologically efficient ferroelectrics because of their intense polarization and numerous phases. Twelve co-ordinated A-cations and six co-ordinated B-cations make up the wide spectrum of perovskite oxides with ABO_3 structure. A cuboid unit cell is typically used to depict the structure, with oxygen anions positioned at the central point of each face, B-cations in the centre, and A-cations at the corners [3, 4]. Ionic displacement and order-disorder transitions cause polar non-centrosymmetry in perovskite ceramic materials, which leads to reversible spontaneous polarization when an external electric field is applied [5]. However, the development of lead-deficient phases delays and impedes the production of perovskite [6,7].

It is strong spontaneous polarization, high pyroelectric coefficient, low dielectric constant, ferroelectric/piezoelectric behaviour, and structural phase transitions as a result of which the polycrystalline perovskite $PbTiO_3$ has attracted ongoing attention. One of the important members of this family is $PbTiO_3$. Because of its many physical characteristics, $PbTiO_3$ has garnered a lot of interest in fundamental research. Because of its high pyroelectric coefficient and comparatively low permittivity, $PbTiO_3$ finds extensive use in electronics, including multilayer capacitors, resonators, and ultrasonic transducers [7, 8]. It is a displacive-type ferroelectric material with the highest tetragonal lattice strain c/a ~ 1.064 in the perovskite titanate. It has a structural phase transition from tetragonal (space group: P4mm) to cubic (space group: $Pm\bar{3}m$) at Curie temperature, T_c ~ 490 °C [9,10]. However, due to its large lattice non-centrosymmetric tetragonal strain in pure $PbTiO_3$, it is difficult to get a dense ceramic form for the use of ferroelectric/ piezoelectric applications [11].

There are various preparation methods that have been exploited to synthesize perovskite $PbTiO_3$ material. Herein, we report perovskite $PbTiO_3$ preparation by solid state route. Since this method provides single phase and control over the preparation in various processing steps, we preferred this very method. We emphasized on the structural, electrical and optical properties to point out its feasibility in modern device applications and possible modifications.

2. EXPERIMENTAL DETAILS

2.1 SAMPLE SYNTHESIS

The lead titanate sample, a well-known ferroelectric material $PbTiO_3$, was made using the traditional solid-state reaction ceramic fabrication method. PbO [Lead (II)] and TiO_2 were the initial analytic grade materials. To create $PbTiO_3$, these solid form powder oxides were combined in stoichiometric proportions. The mixture was calcined in air at 1250 °C for 8 hours after being mechanically ground in agate mortar for 5 hours. Following three hours of grinding at 1300 degrees Celsius, the mixture was once more heated. The resulting double-calcined combination was ground into fine powders, compressed into 10-mm-diameter pellets using a hydraulic press and 8 tonnes of pressure, and then sintered in air at 1350 degrees Celsius. The circular surface of the pellet was polished by silver oxide to for electrode in order to carry out the electrical measurements smoothly.

2.2 CHARACTERIZATIONS

X-ray powder diffraction technique at room temperature is used to identify the crystal structure, type of phase and crystallite size of $PbTiO_3$ powder by means Bruker D8-Advance X-ray diffractometer with Cu$K\alpha_1$ (1.5406 Å) radiation. The data was collected with a step size of 0.02° over the angular range 2θ (20° < 2θ < 80°) generating X-ray by 40 kV and 40 mA power settings. Fourier Transform Infrared Spectroscopy was carried by Perkin Elmer FT-IR/FIR spectrometer (frontier) in the range of 400-4000 cm^{-1}. Dielectric measurements were performed as a function of frequency in the range of 20Hz–1MHz on Novocontrol alpha-A high performance frequency analyzer at room temperature. UV-Vis spectrometer (Perkin Elmer, Lambda 950 - USA) was used to find the band gap of all the samples under investigation.

3. RESULTS AND DISCUSSION

3.1 STRUCTURAL ANALYSIS

The prepared sample $PbTiO_3$ powder has been structurally characterized by X-ray powder diffraction (XRD). XRD was used to determine the phase structure and purity of the as-synthesized sample. Room temperature XRD pattern of the sample is shown in Figure 1.

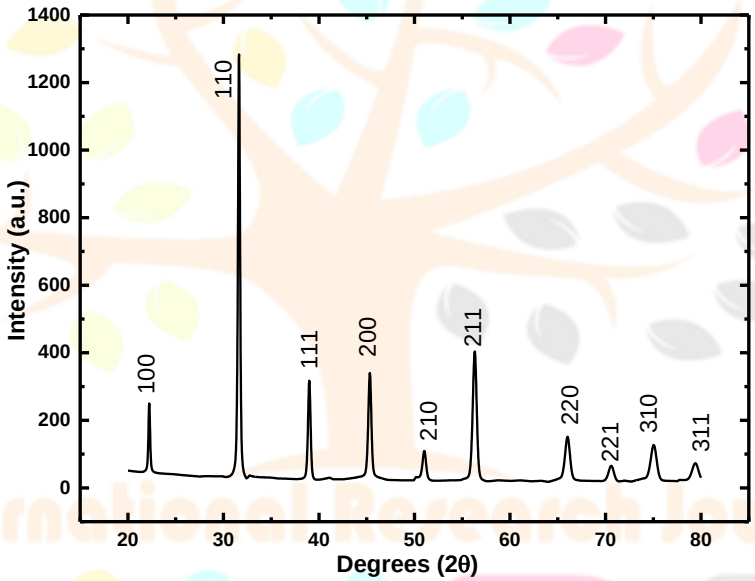

Figure 1: X-ray diffraction pattern of $PbTiO_3$

Analysis of the XRD pattern revealed the tetrahedral structure of the sample with the assigned space group P4mm [12]. The absence of additional diffraction peaks within the experimental limits reveals the purity of the sample. The narrowness of the characteristic XRD peaks is indication of larger average crystallite size whereas the sharpness of these peaks is attributed to the high crystallinity of samples.

The classical Debye-Scherrer's formula [$d = 0.9\lambda/\beta\cos\theta$ where, λ is the wavelength of Cu$K\alpha_1$ radiation used and β is the full width half maximum (FWHM) of the highest intense peak, 2θ is the diffracting angle and 'd' is average particle size of the samples is exploited to calculated the average particle size which comes out to be about 96 *nm*.

3.2. DIELECTRIC MEASUREMENT

3.2.1 DIELECTRIC PERMITTIVITY

Studies have been carried out on $PbTiO_3$ sample to investigate the combined effect on dielectric nature of the sample. The real part (ε') of dielectric constant is the measure of the amount of energy stored in a dielectric due to the applied field and is calculated by using formula $\varepsilon = ct/A\varepsilon_0$ where ε_0 is the permittivity of free space, '*t*' is the thickness of pellet, 'A' is the cross sectional area and '*C*' is the capacitance of pellet. The fluctuation of ε' with frequency at room temperature is depicted in Figure 2. Figure 2 makes it clear that for the prepared sample, the dielectric constant (ε') drops as the frequency (f) increases and becomes constant at higher frequencies. The dispersion caused by Maxwell-Wagner [13] type interfacial polarization is revealed by this fluctuation of ε' with Log*f*, which is consistent with Koop's phenomenological theory [14]. The interfacial dislocations, oxygen vacancies, charged defects, grain boundaries effect, and interfacial/space charge polarization brought on by heterogeneous dielectric structure could all be responsible for the high dielectric constant values at low frequencies [15-17].

3.3.2 DIELECTRIC LOSS (Tanδ)

Figure 3 shows how the loss tangent (tanδ) varies with frequency at room temperature. At high frequencies, the dielectric loss is reduced because domain wall motion is suppressed, and at lower frequencies, the dielectric loss reaches its maximum when the frequency of electron hopping between different ionic sites approaches the frequency of the applied field. The dielectric loss occurs when the polarization lags behind the applied alternating field, which is caused by the presence of impurities

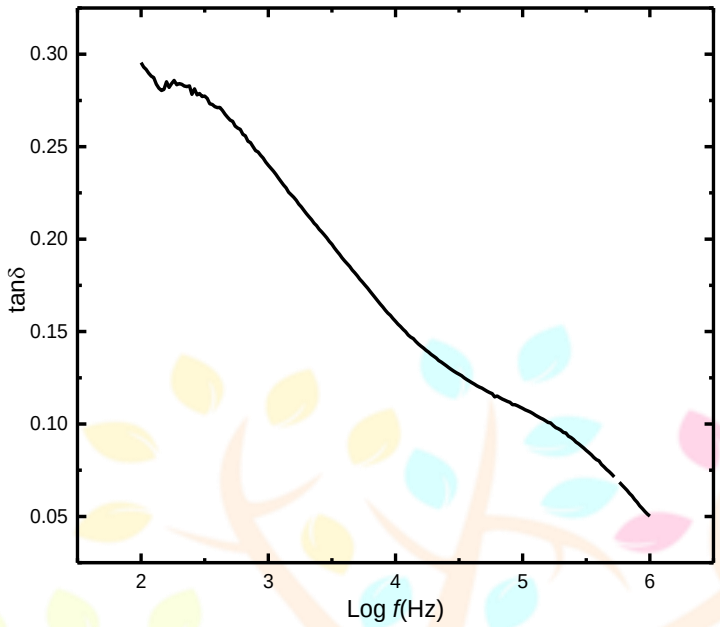

Figure 3: Dielectric loss (tanδ) as a response to the applied frequency at room temperature

The value of dielectric loss tangent is high at low frequency and progressively reduces and attains a constant value at higher frequency region [18]. In the present study, the dielectric loss attains a maximum value at a particular frequency. This characteristic is attributed to the resonance between the applied electric field and the polaron hopping frequency [15-19]. The Intriguing values of Dielectric constant and dielectric loss at low and high frequency are given in the Table 2.

3.2.3 CONDUCTIVITY (σ_{ac})

The ac conductivity $PbTiO_3$ sample's in response to the applied *ac* field is displayed in Figure 4. The extremely low values of conductivity displayed in graph demonstrate the sample's insulating properties. The conductivity resulting from the hole movement is responsible for the low frequency portion of the plot, which is essentially unresponsive to the applied field. The ac conductivity does, however, show growth after a certain applied field limit, after which each increase in the applied field sharply increases the conductivity. When a critical field value is attained, the behaviour is explained in terms of the face that the charge carriers are bound by, including dislocations, defects, inhomogeneities, and the charge centres that are discharged [20,21].

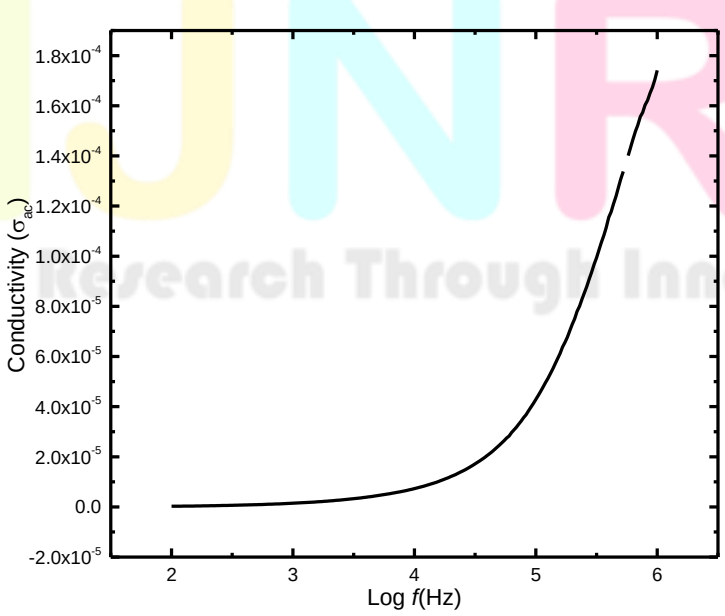

Figure 4: ac conductivity of lead titanate

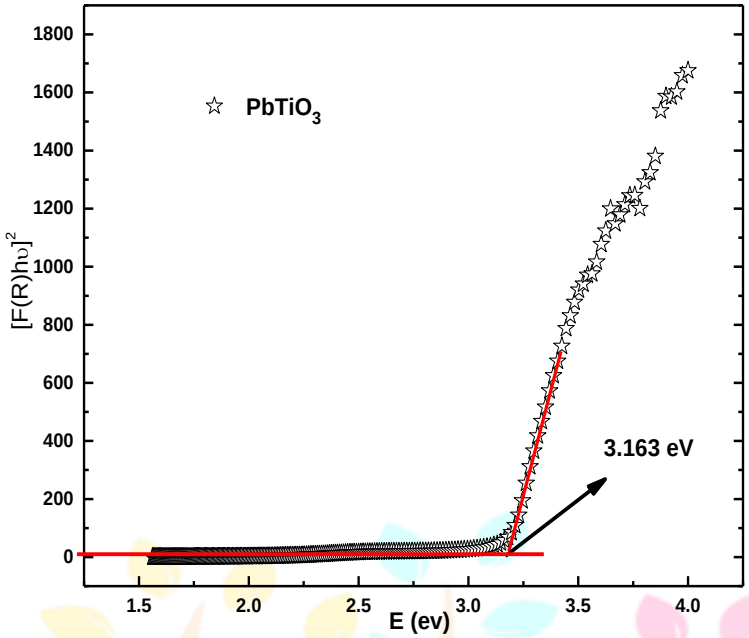

Figure 5: Optical band gap by Tauc's plot of Lead Titanate

3.3 OPTICAL BANDGAP STUDIES

The optical properties of $PbTiO_3$ compound was investigated with the help of diffuse reflectance UV–Vis spectroscopy. The direct band gap (n=2) was determined by plotting $[F(R)h\upsilon]^2$ as functions of energy $E = h\upsilon$ as shown in Figure 5. To estimate approximately the band gap (E_g) of the as prepared materials, we extrapolated the line along the sharp edge of the spectral curve to intercept the energy axis [22-24]. The value of the intercept provides the approximate value of the energy band gap (E_g). The bandgap value of $PbTiO_3$ was found to be 3.163 eV. The higher value of energy bandgap of $PbTiO_3$ material is reported elsewhere [25]. The large energy bandgap value exhibited by $PbTiO_3$ perovskite material indicates the potential applications in semiconductor devices [25,26].

3.4 ELECTRICAL POLARIZATION

The $PbTiO_3$ ceramic material is expected to be good ferroelectric in nature. We examined it for for the polarization behaviour at a field value of 1500V. The P-E loop is shown by the Figure 6. From the loop, it is clear that sample inherits incomplete hysteresis P-E loop that displays conducting nature and hence the leakage and exhibit low polarization values as revealed from the plot [27]. The remnant polarization (P_r) value is of the order of 0.075 μC/cm^2, Ps = 0.175 μC/cm^2 and coercive field (E_c) of the order 2.1 kV/cm. The low polarization effect is believed to arise from poor morphology where grain would have grown with defined grain boundaries associated with uneven size distribution and large separation [27-29]. The results are still intriguing and appeal for the modification in the sense of particle size, preparation process, doping concentration and sintering temperature

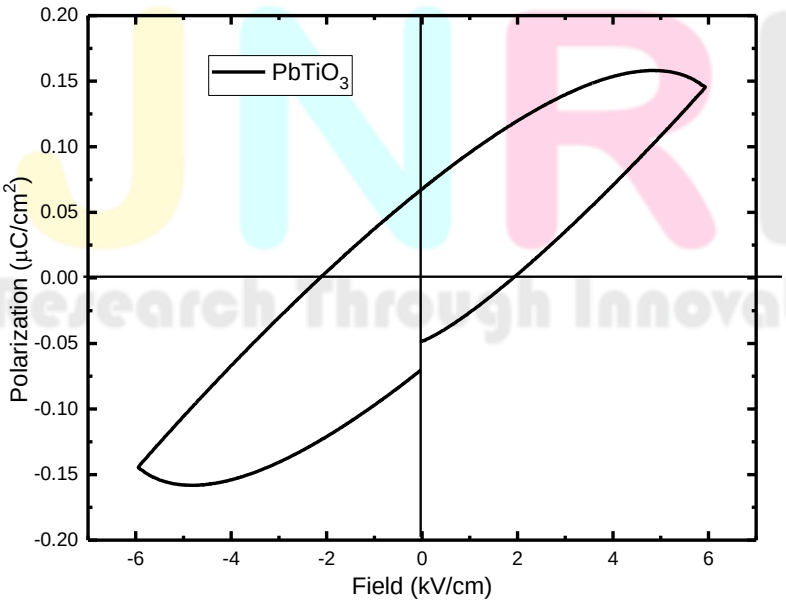

Figure 6: Electric Polarization (P-E Hysteresis loop) of $PbTiO_3$

CONCLUSION

We have successfully prepared a single phased and pure $PbTiO_3$ material using ceramic route i.e. solid state reaction method. XRD analysis confirmed the tetragonal structure acquired by the $PbTiO_3$ sample with space group *P4mm*. The particle size is about 96nm attributed to higher temperature treatment. Furthermore, the sample has been witnessed to be highly crystalline in nature with enhanced grain growth arising from temperature effect. Dielectric measurements reveal that the sample exhibits an admirable dielectric constant which reduces with the increase in the frequency. The same behavior is observed for dielectric loss with increasing in the applied ac field. The wide bandgap characteristics are expected to be useful in multilayer capacitor, resonators, and ultrasonic transducers. Low polarization is witnessed however there is possibility to rectify the P-E hysteresis loop character of the sample. The results seem to be interesting and needs further attention.

ACKNOWLEDGEMENTS

SAGE University is acknowledged for providing research opportunity. UGC-DAE-CSR, as an institute is acknowledged for providing characterization facilities. Al the researchers at SAGE University, Department of physics are extends warm thanks for guidance and Support.

REFERENCES

[1] W.S. Jung, J.H. Kim, H.T. Kim, et al., Mater. Lett. 64 (2) (2010) 170–172.
[2] S. Anwar, P.R. Sagdeo, N.P. Lalla, Solid. State. Sci. 9 (11) (2007) 1054–1060.
[3] H.T. Jiang, J.W. Zhai, M.W. Zhang, et al., J. Mater. Sci. 47 (6) (2012) 2617–2623
[4] P.R. Ren, H.Q. Fan, X. Wang, et al., Int. J. Appl. Ceram. Technol. 9 (2) (2012) 358– 36
[5] K.H. Chen, T.C. Chang, G.C. Chang, et al., Appl. Phys. A-Mater. 99 (1) (2010) 291–295.
[6] H. Chen, C. Yang, C. Fu, et al., J. Mater. Sci-Mater. El. 19 (4) (2008) 379–382.
[7] J. Chen, C. Fu, W. Cai, G. Chen, S. Ran, Journal of Alloys and Compounds 544 (2012) 82–86
[8] X. Wang, J. Wu, B. Dkhil, C. Zhao, T. Li, W. Lia and X. Lou, RSC Adv., 7 (2017) 5813
[9] P. Mishra and P. Sonia Kumar, J. Alloys Compd., 545 (2012) 210–215.
[10] J. Li, D. Zhang, S. Qin, T. Li, M. Wu, D. Wang, Y. Bai, X. Lou, , Acta Materialia, 115 42 (2016) 58-67.
[11] Z. Luo, D. Zhang, Y. Liu, D. Zhou, Y. Yao, C. Liu, B. Dkhil, X. Ren and X. Lou, Appl. Phys. Lett., 105(10) (2014) 102904.
[12] G. Singh, I. Bhaumik, S. Ganesamoorthy, R. Bhatt, A. Karnal, V. Tiwari and P. Gupta, Appl. Phys. Lett., 102(8) (2013) 082902.
[13] P. Wu, X. Lou, J. Li, T. Li, H. Gao, M. Wu, S. Wang, X. Wang, J. Bian, X. Hao, journal of Alloys and Compounds, 725 (2017) 275-282
[14] S.-G. Lu, Q. Zhang, Electrocaloric Materials for Solid-State Refrigeration, Advanced Materials, 21 (2009) 1983-1987.
[15] J.F. Scott, Electrocaloric Materials, Annual Review of Materials Research, 41 (2011) 229-240.
[16] X. Moya, S. Kar-Narayan, N.D. Mathur, Caloric materials near ferroic phase transitions, Nature 6 materials, 13 (2014) 439-450.
[17] A. Sati, A. Kumar, V. Mishra. K. Warshi, A. Sagdeo, S. Anwar, R. Kumar, P. R. Sagdeo, Journal of Materials Science: Materials in Electronics 30 (2019) 8064–8070
[18] Wagner, K.W.: Ann. Phys. 40 (1913) 817
[19] Koops, C.G.: Phys. Rev. 83 (1951) 121
[20] Saleem, M., Mishra, A. and Varshney, D. J. Supercond Nov. Magn. 31 (2018)943
[21] Bergman, R.: J. Appl. Phys. 88 (2000) 1356
[22] Psarras, G.C., Manolakaki, E., Tsangaris, G.M.: Composites A. 34 (2003) 1187
[23] R. Ranjan, R. Kumar and N. Kumar, J. Alloys Compd. 509 (2011).
[24] M. S. Cao, Z. L. Hou and J. Yuan, J. Appl. Phys. 105 (2009). 106102
[25] M. S. Cao, W. L. Song and Z. L. Hou, Carbon 48 (2010) 788
[26] P. B. Macedo, C. T. Moynihan and R. Bose, Phys. Chem. Glasses 13 (1972) 171
[27] Y. Wei and S. Sridhar, J. Chem. Phys. 99 (1993) 3119
[28] W. S. Yan, R. Zhang, Z. L. Xie, X. Q. Xiu, Y. D. Zheng, Z. G. Liu, S. Xu,: Appl. Phys.. Lett. **95**, (2009) 222901
[29] T. Shimada, S. Tomoda, T. Kitamura,: J. Phys.: Condens. Matter **22**, (2010)355901